Methods of Quantifying Susceptibilities in Gel Phantoms

Y-C. N. Cheng[1,2], M. S. Dawood[2], Q. Liu[2], J. Jiang[2], E. M. Haacke[2,3]

[1]Department of Physics, Case Western Reserve University, Cleveland, Ohio 44106-7079, United States, [2]Wayne State University, Detroit, Michigan 48202, United States, [3]The MRI Institute for Biomedical Research, 440 E. Ferry St. Unit 2, Detroit, Michigan 48202, United States

Introduction

Quantifying iron content inside the human body is important because many diseases are associated with iron overload such as Alzheimer's disease, hemochromatosis and Parkingson's disease. Many researchers have measured T2* (or R2*) of different tissues as an indicator of iron content [1]. However, such an approach is good only if the MR signal as a function of echo time decays exponentially. When MR signals show bi-exponential decays [2], one will need to consider the use of a fundamental physical quantity. In this case, the challenge is to measure accurately the averaged susceptibility in a tissue when iron is present. In order to work toward this goal, we first study an experiment when an air tube is in the middle of a gel phantom. The susceptibility difference between the gel and air creates a phase variation in the gel. In this abstract we compare a new approach to measure susceptibility using both magnitude and phase images and compare the results with those from a more conventional phase approach in gel phantoms [3].

Imaging Methods

A capillary tube (Fisher Scientific) was inserted into a rectangular gel phantom of dimensions 139 mm x 109 mm x 64 mm with 0.5 mm uncertainty along each dimension. The tube was parallel to the shortest edge and was inserted in the middle of the phantom. The tubes were then extracted from the phantom. The outer diameter of the tube was directly measured using a micrometer to be 1.615±0.003 mm. The phantom was placed inside a 1.5T Sonata Siemens system such that the remaining cylinder of air was perpendicular to the main field. A low-resolution spin echo sequence was performed in order to slightly adjust the coronal images to be perpendicular to the tube. Two sets of coronal images (with different echo times) from a 3D high resolution fully velocity compensated FLASH sequence were obtained with the following imaging parameters: TR = 50 ms, TE = 5 (and 6) ms, flip angle = 15°, resolution = 1 mm x 1 mm x 1 mm, Nx = 256, Ny = 128, and Nz = 64.

Data Analysis and Results

From the TE = 5 ms coronal sets with only air (Fig. 1), we select 5 phase images that appear to have correct dipole field patterns in the middle slices and 5 other images that do not seem to have the same feature. From pixels along the x-axis in each image, we are able to fit the phase as a function of distance using the $1/r^2$ dipole behavior. The tube center has to be corrected due to the fact that the diameter of the tube is comparable to the image resolution. The phase can be fit directly or by taking the logarithm. Using the latter approach, the center of the tube can be estimated. Near the edge of the tube partial volume effects modify the expected $1/r^2$ dipole behavior. For this reason, pixels near the edge of the tube may need to be excluded. Fitting $1/r^2$ is only valid far from the tube's center but this is just where the error in the phase measurement becomes large (at least for the case of the air tube). The method of error propagation is used to find the uncertainties of our results. The susceptibilities calculated from a total of 10 slices are listed in Fig. 2, when the logarithms of both the phase and distance were taken. Given these difficulties in the phase measurement, we considered a complex integration method. For a long tube, the dephasing effect can be modeled theoretically and an analytical formula obtained. Based on Eq. 1 in [4], it is possible to calculate the susceptibility of the gel when the spin density of the gel and its volume fraction are known. This volume fraction is obtained by choosing a circle around the air tube with its center identical to the tube center (see Fig. 1). The complex signal is then summed over for a series of radiuses (Fig. 3). When the radius of the circle is less than 6 times that of the tube, the gel susceptibility can be accurately estimated from the sum of the complex signals. The results from a particular slice are listed in Fig. 4. The results show a good consistency with reduced error compared to the phase fitting method.

Discussions

The integration method used in the air tube analysis shows great promise to accurately extract the susceptibility of the gel. This method is not limited by the partial volume effect rather it takes advantage of this natural limitation and can be used with the presence of only a few pixels around the tube center. On the contrary, the fitting of the phase to the dipole form $1/r^2$ requires including pixels far from the tube center but suffers from noisy phase data. Of course, in the complex summation approach if the radius chosen over which to integrate the data is too small, the results will be noisy as well. Our results have shown that with a volume fraction from 0.28 (radius 1.5 mm) to 0.018 (radius 6 mm), the susceptibilities agree to within 5%. The results for air in gel (mainly water) are in good agreement with the expected value of about -10 ppm, which is consistent with a -10.02 ppm susceptibility measured experimentally from a 5 M NaCl solution [5].

Fig. 1: An example coronal phase image of the air tube inside the gel phantom.

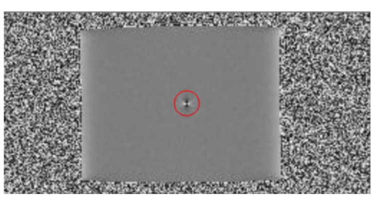

Fig. 2: A plot of susceptibilities from 10 coronal slices using the least square fit of the phase images.

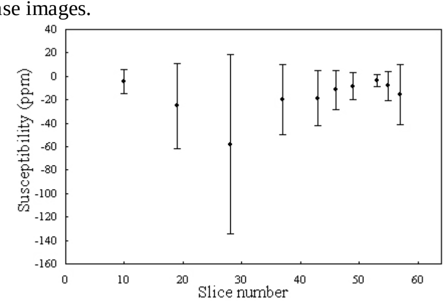

Fig. 3: Magnitude of the complex sum as a function of radius. The solid curve is the theoretical simulation with the susceptibility chosen to be -10 ppm.

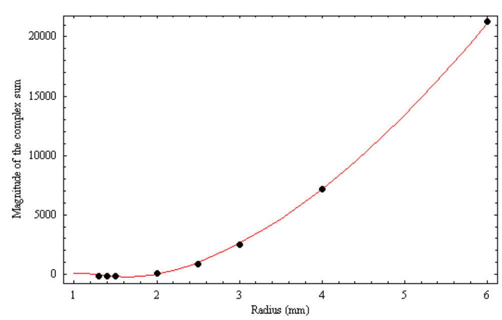

Fig. 4: A plot of susceptibilities calculated from slice no. 43 in Fig. 2 using the integration method. The tube center is chosen at the (64.4, 128.7) pixel.

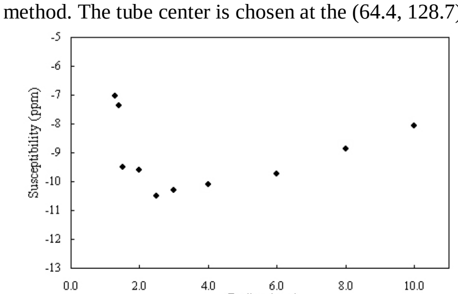

References

[1] Vymazal et al., JMRI 5: 554-560; 1995.
[2] Gelman et al., Radiology 210: 759-767; 1999.
[3] Weisskoff et al., MRM 24: 375-383; 1992.
[4] Cheng and Haacke, NMR in Biomedicine, 14: 468-477, 2001.
[5] Chu et al., MRM, 13: 239-262, 1990.